Journal of Computers Vol. 33 No. 3, June 2022, pp. 113-123
doi: 10.53106/199115992022063303009

Automatic Detection and Localization of Pulmonary Nodules in CT Images Based on YOLOv5

Chun-Man Yan, Cheng Wang*

College of Physics and Electronic Engineering, Northwest Normal University, Lanzhou 73007, China
yancha02@163.com, 610487244@qq.com

Received 29 July 2021; Revised 14 November 2021; Accepted 14 December 2021

Abstract. Lung cancer has always threatening human health and life. As small pulmonary nodules are main early features of lung cancer, early screening for small pulmonary nodules through computed tomography (CT) imaging is essential for the treatment of lung cancer. In this paper, the YOLOv5 model is improved to improve the ability of detection and recognition of small pulmonary nodules in complex CT lung images. Firstly, the preprocessing step is put into effect to obtain the lung parenchyma in CT images. Then, the backbone structure of YOLOv5 is improved by iResNet to improve the ability of feature extraction, and the feature fusion network is improved by BiFPN to improve the detection ability of small pulmonary nodules. Finally, the strategy of group normalization is used to improve the model performance under small batch size training condition. The experimental results on LUNA16 data set show that the detection AP of the improved model reach 94.8%, the competitive index score is 0.895, and the sensitivity is 78.1%, 94.4%, under 1/8 and 1/4 FPs, respectively. Compared with other two-dimensional target detection models, the improved yolov5 model has better detection ability of small pulmonary nodules. And, the results are better than most other two-dimensional pulmonary nodule detection methods. In addition, compared with other three-dimensional pulmonary nodule detection methods.

Keywords: deep learning, computer-aided detection (CAD), YOLO v5, pulmonary nodule

1 Introduction

Lung cancer, as one of the cancers with the highest morbidity and mortality in the world, has always threatened people's health and life [1]. Pulmonary nodules are an important symptom for early diagnosis of lung cancer, which can be effectively found by using low-dose computed tomography (CT). However, in clinical practice, a patient will generate a large number of CT sequences, and most of the pulmonary nodules are small and distribution complex, so radiologists are easy to miss the diagnosis. Therefore, the prediction result of computer aided diagnosis (CAD) can be used as the second diagnosis result to help radiologists diagnose lung cancer, which can effectively improve the accuracy of lung cancer diagnosis. Therefore, Research on CAD of pulmonary nodules has very important clinical significance and research value.

Pulmonary nodule CAD system generally consists of two stages: (1) candidate nodule detection; (2) false positive reduction. In the first stage, in order to improve the sensitivity of pulmonary nodule detection, a large number of pulmonary nodule candidate regions are screened out from CT images. In the second stage, a classifier is designed to remove a large number of false positive results. Traditional CAD pulmonary nodule detection method [2] firstly extracts suspicious tuberculosis by morphological method, and then uses support vector machine (SVM) and other classifiers to classify suspicious nodules. For example, Campadelli et al. [3] used a multi-scale filter to find the circular region, and then classified the candidate nodules by SVM. But it has poor detection effect for irregular pulmonary nodules. Giger ML et al. [4] used multi threshold algorithm to detect pulmonary nodules. However, the gray value range of nodules is similar to that of other tissues such as chest wall and blood vessels. Therefore, resulting in high false positive. The traditional CAD system has some problems, such as complicated pretreatment steps and high false positive rate, it is difficult to apply in clinical practice.

In recent years, detection of pulmonary nodules CAD system based on convolutional neural network (CNN) has developed rapidly. It is divided into two-dimensional CNN (2D-CNN) detection model and three-dimensional CNN (3D-CNN) detection model. For example, Li et al. [5] introduced the inception V3 module into YOLO v2 network to obtain a pulmonary nodule detection network suitable for 2D images, which can effectively extract the multi-scale features. Ding et al. [6] combined three adjacent CT sequences into one 2D image, and used the

* Corresponding Author

improved Faster R-CNN network to detect pulmonary nodules, which can make more effective use of the features of pulmonary nodules. Miao et al. [7] proposed an improved network model structure based on U-Net, which can fuse semantic features and low-level features of pulmonary nodules to improve detection ability. Although these methods improve the feature extraction ability of pulmonary nodules, the method based on 2D CNN still can't make full use of the feature information of pulmonary nodules, so its performance has a bottleneck. However, the detection model base 3D CNN can learn the 3D features of pulmonary nodules, which is helpful for the detection and classification of pulmonary nodules. For example, Khosravan et al. [8] used 3D SSD and Dense Blocks to build a single-stage pulmonary nodule detection model, which improved the speed of pulmonary nodule detection. Liu et al. [9] extended the 2D CNN structure of FPN network into3D CNN, and used dense connection for multi-scale feature fusion. This method improved the detection ability of multi-scale pulmonary nodules. Although the detection accuracy based on 3D CNN model is high, the time complexity is high, it has high time complexity and high requirements for hardware resources compared with 2D CNN. In addition, due to the different imaging quality of different CT equipment, the preprocessing steps of 3D CNN are more complex. On the contrary, 2D CNN does not have the above problems. Therefore, using 2D image information to detect pulmonary nodules is an ideal method. However, when the original target detection model is directly applied to pulmonary nodule detection, the false positive results are very high, especially the missed detection rate of small nodules is very high.

Therefore, this paper proposes an improved YOLOv5 pulmonary nodule detection algorithm. The mainly contributions include: 1) In order to solve the imaging quality of different CT equipment in CT images on the detection effect. Pretreatment methods such as lung parenchyma segmentation were used; 2) In order to improve the feature extraction ability of model for pulmonary nodules, the backbone of YOLOv5 is improved by introducing ResBlock unit of iResNet in different feature extraction stages; 3) In order to improve the detection ability of the network for small pulmonary nodules. Adopting the idea of BiFPN, a cross level feature fusion mode is added on the basis of the original feature fusion network to improve the feature fusion network ofYOLOv5; 4) Improve the BN in the model with GN to improve performance when using the small batch size training model. Finally, the improved YOLOv5 model is trained on LUNA16 data set through small batch size. Experimental results show that this method has higher detection accuracy and sensitivity than other 2D CNN target detection models. And, this method has better sensitivity under most false positive rates, and the competitive index is better than other 2D CNN methods. In addition, compared with other 3D CNN pulmonary nodule detection methods, this method also has better comprehensive performance.

The rest of this paper is organized as follows. Section 2 describes the working principle and research methods of this method in detail. In Section 3, the experimental results on LUNA16 are presented and compared with the reported methods. And in Section 4, conclusion and discussion of the work are given.

2 Methods

2.1 LUNA16 Dataset Preprocessing

The preprocessing step of dataset includes resampling and normalization of the original CT image. The former solves the problem of inconsistent image resolution from different CT scanning equipment, while the latter solves the problem of inconsistent gray information of the same tissue.

2.1.1 Resampling of the Original CT Image

Different CT equipment scan images with different pixel sizes and granularity. For example, the pixel interval of one scanning slice can be [2.5, 0.725, 0.725], that is, the distance between slices is 2.5 mm, and the other scanning slice may be [1.5, 0.5, 0.5]. Therefore, we resample the original CT images in three directions (coronal plane, sagittal plane and cross section) with fixed 1×1×1(mm) pixels, so that the same detection model can adapt to CT scanning images from different equipment.

2.1.2 Normalization Processing

The images in LUNA16 dataset come from different CT equipment, which leads to gray differences in CT images and interferes with pulmonary nodule detection. Therefore, it is necessary to remove the interference caused by different pixel value as much as possible before the procedure of transforming CT images into gray images.

Because the Hounsfield Unit (HU) value of the pulmonary is about -500. Therefore, the data near the lung HU value [-1000, 400] is reserved (from air to bone), and the HU value beyond this range is discarded. In this paper, the linear function transformation method is used to normalize the images, and the calculation method is as follows:

$$N'_{(m,n)} = \frac{N_{(m,n)} - HU_{min}}{HU_{max} - HU_{min}} \quad (1)$$

where $N_{(m,n)}$ and $N'_{(m,n)}$ are the values before and after normalization. HU_{min}, HU_{max} are the minimum HU value of -1000 and the maximum HU value of 400 respectively. After normalization, the CT slices with the pulmonary nodule center are extracted to construct the data, with a total of 1186 images.

2.2 Pulmonary Parenchyma Segmentation

Pulmonary CT images are mainly composed of air, organs, bones, muscles and pulmonary parenchyma, and pulmonary nodules only exist in pulmonary parenchyma. In order to improve the accuracy of detection and reduce the detection time, pulmonary parenchyma segmentation is performed first, and the areas outside the boundary of both lungs are removed from CT image.

The pulmonary parenchyma segmentation process in this paper is shown in Fig. 1. Where a is the original CT slice image; b is the slice gray image; c is the image after threshold segmentation; d is the image after closed operation; e is pulmonary mask; f is the image of pulmonary parenchyma.The steps are as follows: 1) Transform CT image slices into gray-scale images; 2)Segmenting gray image by global adaptive threshold method; 3) Adopting the close operation in morphology to remove the Granular areas and the maps of blood vessels; 4) Using the maximum connected component method to obtain the pulmonary contour and the lung mask; 5) Carrying out the mask calculation for pulmonary parenchyma mask and gray image to obtain the final segmentation of pulmonary.

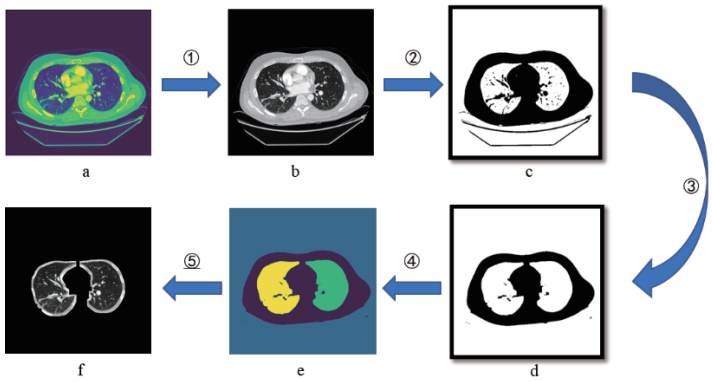

Fig. 1. Pulmonary parenchyma segmentation process

2.3 Pulmonary Nodule Detection Network

The improved pulmonary nodule detection network is shown in Fig. 2. On the basis of YOLO v5, firstly, the backbone of YOLO v5 is improved by ResBlock unit of iResnet [10], then the fusion mode of feature fusion network is improved by BiFPN, and finally all Batch Normalization (BN) in the network is replaced by Group Normalization (GN).

2.3.1 Group Normalization

Batch Normalization (BN) reduces the difficulty of model training and alleviates the problem that the model is difficult to converge due to the disappearance of gradient. However, BN needs a large enough batch size to achieve remarkable results. In order to improve the detection ability of pulmonary small nodules, the algorithm in this paper scales CT images to 640*640 size during training, which leads to the need of large GPU memory during training and the inability to use large batch size for training.

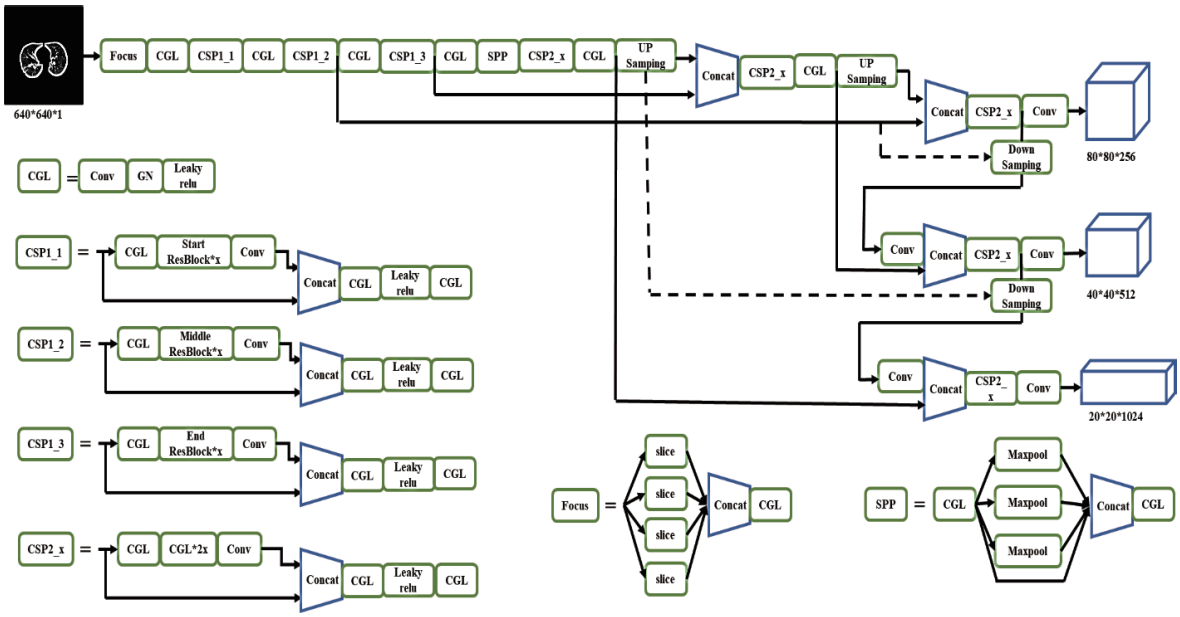

Fig. 2. Improved the network structure of YOLOv5

Therefore, group normalization (GN) [11] is used to improve BN in YOLOv5 and improve the performance of small batch size training model. Comparison between BN and GN is shown in Fig. 3. The input data of neural network usually has four dimensions: B (batch), C (channel), H (height), and W (width). In the training process, the data of each batch that can be stored in GPU memory are limited. BN is calculated in batch size dimension of N size. When calculating the mean and standard deviation, GN divides the dimension C of each characteristic channel into G groups, and then there are C/G channels in each group, and then calculates the mean and standard deviation of each group. Because GN does not depend on batch size, GN can effectively stabilize the gradient changes in the training process and prevent gradient dispersion when using the small batch size training model.

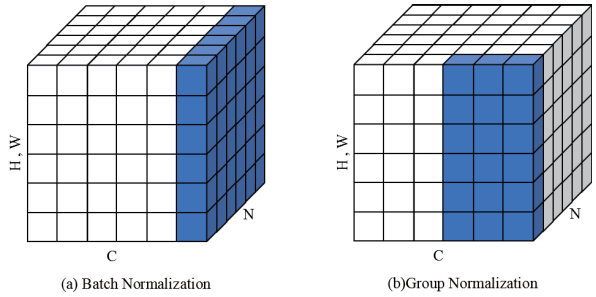

Fig. 3. Two ways of normalization

2.3.2 Backbone

A CSP structure is designed in CSPDarkNet, the backbone network of YOLOv5. Its main unit is built by ResBlock stack with equal mapping capability in Resnet, and its structure is shown in Fig. 4(a). However, the Relu activation function that zeroes the negative signal exists in the main path of ResBlock, and the number of Relu increases linearly with the network depth. This will make the feature information on the main path lost during network training, and increase the difficulty of detecting small nodules.

Therefore, this paper puts forward the structure of Start ResBlock, Middle ResBlock and End ResBlock, which are suitable for different stages of the network, and their structures are shown in Fig. 4. At first, the Relu activation function in the main path of ResBlock is removed in the early and middle stage to improve the problem of feature information propagation. The main path reduces the number of Relu activation function, which greatly limits the learning ability of the model. Therefore, End ResBlock is adopted in the later stage of backbone, and

normalization unit and Relu are added after addition operation, which enhances the nonlinear expression ability of the model. In addition, in order to reduce the computation of 3×3 convolution layer, ResBlock forms a "compression-expansion" structure in the channel dimension through 1×1 convolution layer, which reduces the number of channels but limits the feature learning ability of the model. Therefore, the three-stage ResBlock proposed in this paper no longer reduces the channel dimension, and adopts grouping convolution to reduce the parameters of 3×3 convolution layer, so that the model has enough feature expression ability. The final three ResBlock structures suitable for different stages are shown in Fig. 4(b) Start ResBlock; Fig. 4(c) Middle ResBlock; Fig. 4(d) End ResBlock, where Xi and Xo are the input and output features of the residual block, respectively.

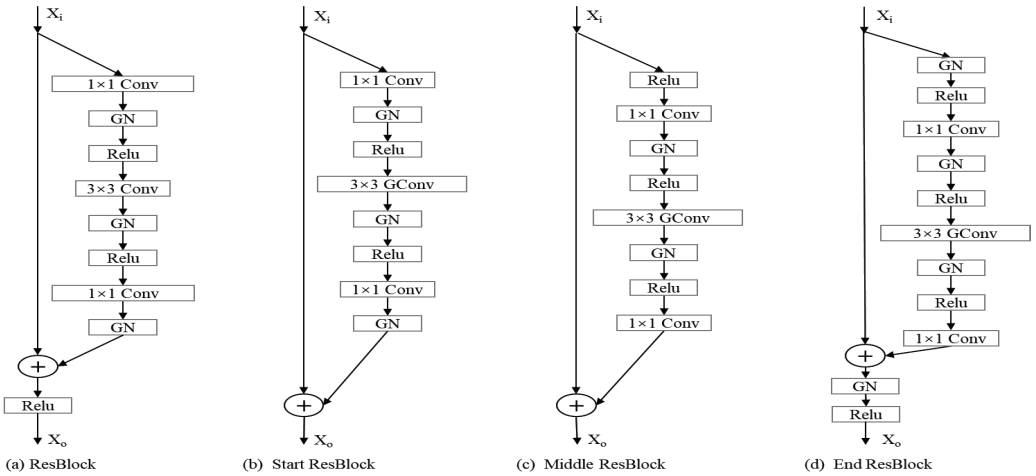

Fig. 4. The ResBlock structure

In the front, middle and back stages of the backbone network of YOLOv5, a CSP structural unit containing ResBlock is included respectively. We use Start ResBlock, Middle ResBlock and End ResBlock instead of ResBlock in the original network to form a new backbone network, which enhances the feature extraction ability of the backbone network for small pulmonary nodules.

2.3.3 Backbone

Feature fusion can make full use of the pulmonary nodule feature information of multi-scale feature map. In the input image, the target of pulmonary nodules is very small. Although the semantic information of pulmonary nodules is getting richer and richer in the process of network forward propagation, the resolution of feature map is getting lower and lower. Especially for small pulmonary nodules, the size of 32×32 pixels of pulmonary nodules in the original image is only 1×1 pixel after five times down sampling, so the detection accuracy of pulmonary nodules using semantic rich deep feature map is very low.

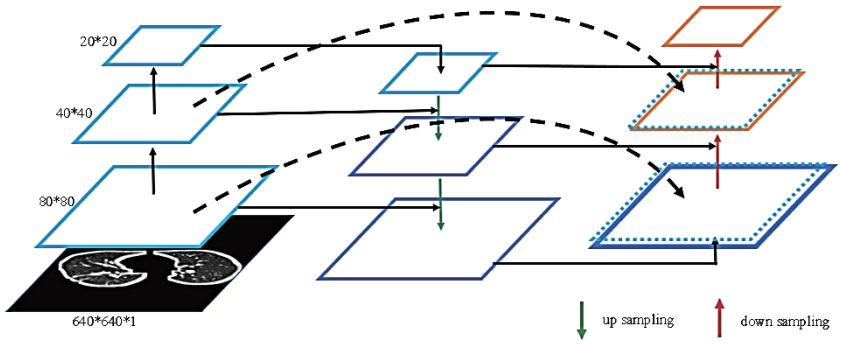

Fig. 5. Improved feature fusion network

Although YOLO v5's feature fusion network has the ability of feature aggregation. However, there are up-sampling and down-sampling operations in the fusion process, which will inevitably destroy the original features of pulmonary nodules. In order to keep the feature information of pulmonary nodules in the original feature map, this paper improves it according to the feature fusion path of BiFPN [12]. The improved feature fusion path is shown in Fig. 5. Cross-level data flow is added between feature maps of the same level, and the original feature map of the same level is added with the feature map fused by PANet, and then down sampling is performed. This method protects the original feature information to the greatest extent, and effectively improves the detection ability of small nodules.

2.3.4 Loss Function

The prediction error of this algorithm is divided into two parts, one is whether the candidate area contains pulmonary nodule classification error, the other is the regression error between the center point position of the candidate area and the offset of pulmonary nodule position. In this paper, we used the binary cross entropy loss as the classification error, and GIoU as regression error. The binary cross entropy loss function is defined as (2):

$$L_{cls}\left(p_i, y_i\right) = -y_i \, log \, p_i - \left(1 - y_i\right) log\left(1 - p_i\right). \tag{2}$$

where y_i is the label value of the i_{th} sample, 0 means background, and 1 means target. p_i indicates the predicted classification probability of whether the sample belongs to the target or the background. The GIoU loss function is calculated as (3):

$$L_{reg} = 1 - GIoU = 1 - \left(\frac{b_{A \cap B}}{b_{A \cup B}} - \frac{\left| b_D / b_{A \cup B} \right|}{\left| b_D \right|} \right). \tag{3}$$

where $b_{A \cap B}$ is the overlapping area, $b_{A \cup B}$ is the total enclosed area, and b_D is the smallest bounding area between the real box and the preselected box, respectively. The total error is combined as (4).

$$L = L_{cls} + L_{reg}. \tag{4}$$

3 Experiments and Analysis

3.1 Dataset and Experimental Platforms

This paper dataset comes from the 2016 Lung Nodule Analysis Challenge in the United States [13]. LUNA16 data set contains only 1186 positive nodules with diameters larger than 3 mm, and a total of 888 3D lung CT image. Firstly, 888 3D lung CT images are preprocessed by resampling and normalization, and then the Z-axis slice where the center of pulmonary nodule is located is extracted, and the experimental data set is formed by lung parenchyma segmentation, which contains 1186 images.

In LUNA16 dataset, csv file marks the position of pulmonary nodules relative to origin in CT scanner coordinate system. Therefore, it is necessary to convert the 3D coordinates into the coordinates in the 2D image, and further calculate the coordinate data needed by xml file in the standard Pascal VOC data format. The coordinate conversion formula is expressed as follows:

$$x' = \frac{x - o_x}{S_x}, y' = \frac{y - o_y}{S_y}, \tag{5}$$

$$w = \frac{r}{S_x}, h = \frac{r}{S_y}, \tag{6}$$

$$x_{min} = x^{'} - \frac{w}{2}, y_{min} = y^{'} - \frac{h}{2}, x_{max} = x^{'} + \frac{w}{2}, y_{max} = y^{'} + \frac{h}{2}. \quad (7)$$

where o_x, o_y is the original point position in the coordinate system of CT scanner, and (x, y) are the coordinate positions of pulmonary nodules marked in csv file. S_x and S_y are the element spacing of CT image in x and y axes. r is the nodule size. x', y', w, h is the central coordinate, width and height of pulmonary nodules in the 2D image, respectively. (x_{min}, y_{min}) is upper left corner coordinate and (x_{max}, y_{max}) is lower right corner coordinate of pulmonary nodules in the 2D image are calculated by formula (7). Finally, the image file and the annotation file are formed into a standard Pascal VOC format data set. According to the ratio of 7:2:1, the data set is divided into training set, verification set and test set as the experimental data set in this paper.

The computer hardware platform GPU used in this paper is NVIDIA GTX1066 and the operating system is Ubuntu16.04. The Pytorch1.7.0 deep learning framework is adopted. The batch size is 8, the initial learning rate is 0.01, the attenuation coefficient is 0.1, and the total number of training rounds is 300. The optimization algorithm adopts SGD, and the momentum factor parameter is 0.9.

3.2 Evaluations Metrics

In this paper, average precision (AP), free receiver operating characteristic (FROC) curve and competition performance metric (CPM) are used as evaluation indexes. The expression of Precision and Recall are described as follows:

$$Percision = TP/(TP + FP), \quad (8)$$

$$Recall = TP/(TP + FN). \quad (9)$$

where TP, FP and FN are the detected number of True Positive cases, False Positive cases, and False Negative cases, respectively. The AP represents the area enclosed by Precision and Recall curves. The formula is as follows:

$$AP = \int_0^1 P(r)dr. \quad (10)$$

The FROC curve takes 7 average false positive rates (FPs) (1 / 8, 1 / 4, 1 / 2, 1, 2, 4, 8) as abscissa under different pulmonary nodule scoring thresholds, and the sensitivity of nodule detection model as ordinate, where sensitivity=Recall.

The CPM value is the average of the detection sensitivity under 7 FPs.

3.3 Results and Discussion

In order to verify the performance of the proposed network, we first compare with the detection method based on 2D-CNN (YOLOv3, YOLOv3-tiny, YOLOv5-s, YOLOv5-m, the Faster-RCNN network with Resnet101 and VGG16) by AP [14-15], sensitivity and average detection speed indicators [16]. The results are shown in Table 1.

Table 1. Comparison for different algorithms

Algorithm	AP/%	Sensitivity/%	Speed/ms
YOLOv3-tiny	65.1	83.5	8.3
YOLOv3	78.6	88.3	27.2
YOLOv5-s	73.9	61.8	14.4
YOLOv5-m	87.7	79.6	29.1
Faster-RCNN (ResNet101)	79.2	91.6	217.4
Faster-RCNN (VGG16)	81.4	90.7	142.8
Our	94.8	96.3	29.9

It can be seen from Table 1 that our method can achieve good results in AP and sensitivity while maintaining a more ideal detection speed. The AP is 94.8%, and the sensitivity is 96.3%. Compared with YOLOv3-tiny and YOLOv3, the improved yolov5 has a stronger backbone network structure and feature fusion network, which can better extract the features of pulmonary nodules, which can better extract the features of pulmonary nodules. The AP is increased by 29.7% and 16.2% and the sensitivity is increased by 12.8% and 8.0%, respectively. However, due to the increase of parameters, the detection speed decreases obviously, but it can still be detected in real time.

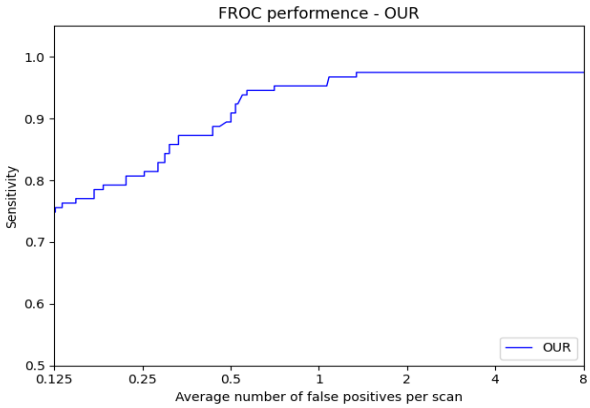

Fig. 6. FROC curve

Compared with the YOLOv5-s, they are greatly improved by 20.9% and 34.5%, respectively. Compared with the YOLOv5-m, this method improves the backbone network structure and adopts the more complex feature fusion structure of BiFPN, so it increases a very short detection time. However, the feature fusion method is more conducive to the detection of small pulmonary nodules. The AP and Sensitivity are increased by 7.1% and 16.7%, respectively. Although the two-stage detection algorithm speed of fast RCNN is much lower than that of YOLO series algorithms. However, its AP and sensitivity have achieved good detection results, with AP reaching 79.2% and 81.4%, sensitivity reaching 91.6% and 90.7% respectively, but still worse than the algorithm in this paper.

The FROC curve of the improved pulmonary nodule detection model is shown in Fig. 6. It can be seen that the sensitivity of the model steadily increases, finally reaching 96.3%. Table 2 shows the sensitivities of 2D-CNN-based method at: 1/8, 1/4, 1/2, 1, 2, 4 and 8 FPs per patient and the CPM score. From Table 2, it can be seen that the pulmonary nodule detection sensitivity of our method are 0.781, 0.799, 0.944, 0.963, and 0.963 at 1/8, 1/4, 1, 2, and 4FPs, respectively. And the CMP reaches 0.895. At 1/8FPs, our algorithm has high sensitivity. At 1/4FPs, the sensitivity of each 2D CNN method is greatly improved. The method in Ref. [15] method obtains the sensitivity close to that of our algorithm. At 1/2FPs, the sensitivity of method in Ref. [15] slightly exceeds that of our algorithm, but at 1FPs, our algorithm is much better than other detection methods. At 2FPs, our algorithm has achieved high sensitivity, while other detection methods have achieved better sensitivity at 8FPs. Therefore, when the false positive rate is very low, our algorithm can obtain high sensitivity and have good detection ability for pulmonary nodules. Therefore, the performance of this algorithm is higher than other detection methods based on 2D CNN.

Table 2. Comparison of pulmonary nodules detection based on 2D-CNN method

	Sensitivity of false positives (FPs) per image							
Method	1/8	1/4	1/2	1	2	4	8	CMP
Ref. [17]	0.692	0.710	0.809	0.863	0.895	0.914	0.923	0.838
Ref. [18]	0.493	0.688	0.796	0.852	0.864	0.864	0.864	0.775
Ref. [19]	0.720	0.735	0.825	0.863	0.901	0.911	0.932	0.841
Ref. [20]	0.690	0.797	0.860	0.900	0.935	0.954	0.977	0.873
Our	0.781	0.799	0.854	0.944	0.963	0.963	0.963	0.895

Table 3 reports the comparison results between the algorithm in this paper and some pulmonary nodule detection methods based on 3D CNN in LUNA16 Challenge. It can be seen that when FPS < 1, JianPeiCAD's

method based on 3D CNN is significantly better than that based on 2D CNN, because it can make better use of the spatial feature information of pulmonary nodules. However, our algorithm has better sensitivity than other 3D CNN methods. When FPS = 1, the sensitivity of our method is close to that of JianPeiCAD's method. All in all, although the overall performance of our algorithm is weaker than that of JianPeiCAD's 3D CNN method, our method has better sensitivity than other 3D CNN methods. So, this algorithm still has a certain competitiveness.

Table 3. Comparison of pulmonary nodules detection based on 3D-CNN method

Teams	Sensitivity of false positives (FPs) per image							
	1/8	1/4	1/2	1	2	4	8	CMP
JianPei CAD	0.848	0.916	0.947	0.961	0.965	0.966	0.967	0.939
Resnet (QiDou)	0.659	0.745	0.819	0.865	0.906	0.933	0.946	0.839
MOT_M5Lv1	0.597	0.670	0.718	0.759	0.788	0.816	0.843	0.742
VisiaCTLung	0.577	0.644	0.697	0.739	0.769	0.788	0.793	0.715
Our	0.781	0.799	0.854	0.944	0.963	0.963	0.963	0.895

The detection effect of the improved model in this paper on three typical pulmonary nodule images (vascular adhesion nodules, isolated small nodules and adherent nodules) are shown in Fig. 7. The upper are the gray images from CT slice, and the lower are the detection results after pulmonary parenchyma segmentation. The results show that our method can detect various types of pulmonary nodules accurately, even for small nodules also with high accuracy.

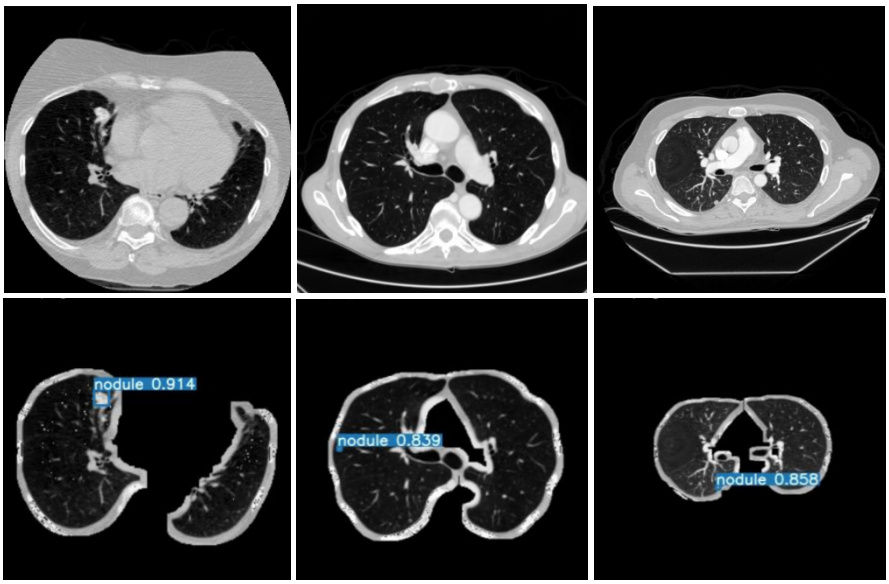

(a) Vascular adhesion nodules (b) Isolated small nodules (c) Adherent nodules

Fig. 7. Detection results of three types of pulmonary nodules

4 Conclusion

To solve the problem of pulmonary nodule detection in medical images, this paper proposes a new computer-aided pulmonary nodule detection method based on YOLOv5. Firstly, to solve the problem of uneven image quality from different medical equipment, a pulmonary image data preprocessing process is proposed. Then an improved model based on YOLOv5 for the detection. The method improves the backbone, feature fusion network and normalization. This algorithm makes full use of the feature information of all nodules and non nodules, and improves the learning ability of the network model for features under small batch size. Compared with the current 2D CNN detection model, this algorithm has better detection ability and sensitivity of pulmonary nodules, and has better detection speed. And compared with other 2D CNN pulmonary nodule detection algorithms, this algorithm can learn and use the characteristics of pulmonary nodules more, and its overall performance is better. In addition,

compared with the 3D CNN pulmonary nodule detection algorithms, this algorithm effectively improves the detection efficiency of nodules and reduces the use of computing resources. In the case of limited hardware resources, this algorithm also has good detection performance and clinical application potential.

In order to improve the detection ability of our algorithm for pulmonary nodules, so as to have better application in diagnosis. In further research, the focus is to establish a 2D CNN model for automatically classifying nodules in the false positive reduction stage of pulmonary nodule detection. In addition, it is necessary to further study the method of extracting the same lung nodule feature information from multiple 2D images to enhance the nodule feature, and further optimize the model to improve the detection ability of pulmonary nodules.

4 Acknowledgement

This work was funded by the National Natural Science Foundation of China (Grant No. 61861041) and the National Natural Science Foundation of China (Grant No. 61961037) and the Industrial Support Plan Project of Gansu Provincial Department of Education (Grant No. 2021CYZC-30).

References

[1] L. Nie, L. Zhang, Y. Yang, Beyond doctors: Future health prediction from multimedia and multimodal observations, in: Proc. the 23rd ACM international conference on Multimedia, 2015.
[2] W.-J. Choi, T.-S. Choi, Automated pulmonary nodule detection based on three-dimensional shape-based feature descriptor, Computer Methods & Programs in Biomedicine 113(1)(2014) 37-54.
[3] P. Campadelli, E. Casiraghi, D. Artioli, A fully automated method for lung nodule detection from posteroanterior chest radiographs, IEEE transactions on medical imaging 25(12)(2006) 1588-1603.
[4] M.-L. Giger, K.-T. Bae, H. MacMahon, Computerized detection of pulmonary nodules in computed tomography images, Investigative Radiology 29(4)(1994) 459-465.
[5] X.-Z. Li, W. Jin, G. Li, C.-Q. Yin, YOLO V2 Network with Asymmetric Convolution Kernel for Lung Nodule Detection of CT Image, Chinese Journal of Biomedical Engineering 38(4)(2019) 401-408.
[6] J. Ding, A. Li, Z. Hu, Accurate pulmonary nodule detection in computed tomography images using deep convolutional neural networks, in: Proc. International Conference on Medical Image Computing and Computer-Assisted Intervention, 2017.
[7] F. Mao, W. Qian, J. Gaviria, Fragmentary window filtering for multiscale lung nodule detection: preliminary study, Academic Radiology 5(4)(1998) 306-311.
[8] N. Khosravan, U. Bagci, S4ND: single-shot single-scale lung nodule detection, in: Proc. International Conference on Medical Image Computing and Computer-Assisted Intervention, 2018.
[9] J. Liu, L. Cao, O. Akin, 3DFPN-HS: 3D Feature Pyramid Network Based High Sensitivity and Specificity Pulmonary Nodule Detection, in: Proc. International Conference on Medical Image Computing and Computer-Assisted Intervention, 2019.
[10]I.-C. Duta, L. Liu, F. Zhu, Improved residual networks for image and video recognition, in: Proc. 2020 25th International Conference on Pattern Recognition, 2021.
[11]Y. Wu, K. He, Group normalization, in: Proc. of the European conference on computer vision, 2018.
[12]M. Tan, R. Pang, Q.-V. Le, Efficientdet: Scalable and efficient object detection, in: Proc. of the IEEE/CVF Conference on Computer Vision and Pattern Recognition, 2020.
[13]A.-A.-A. Setio, A. Traverso, B.-T. De, Validation, comparison, and combination of algorithms for automatic detection of pulmonary nodules in computed tomography images: the LUNA16 challenge, Medical Image Analysis 42(2017) 1-13.
[14]A. Farhadi, J. Redmon, Yolov3: An incremental improvement, in: Proc. Computer Vision and Pattern Recognition, 2018.
[15]S. Ren, K. He, R. Girshick, Faster r-cnn: Towards real-time object detection with region proposal networks, IEEE transactions on pattern analysis and machine intelligence 39(6)(2016) 1137-1149.
[16]K. Xu, H. Jiang, W. Tang, A New Object Detection Algorithm Based on YOLOv3 for Lung Nodules, in: Proc. Proceedings of the 2020 6th International Conference on Computing and Artificial Intelligence, 2020.
[17]A.-A.-A. Setio, F. Ciompi, G. Litjens, Pulmonary nodule detection in CT images: false positive reduction using multi-view convolutional networks, IEEE Transactions on Medical Imaging 35(5)(2016) 1160-1169.
[18]H. Xie, D. Yang, N. Sun, Automated pulmonary nodule detection in CT images using deep convolutional neural networks, Pattern Recognition 85(2019) 109-119.
[19]R.-A. Liu, L.-B. Liu, Detection of Pulmonary Nodules Based on Improved Full Convolution Network Model, Laser & Optoelectronics Progress 57(16)(2020) 161015.

[20]C. Liu, S.-C. Hu, C. Wang, Automatic detection of pulmonary nodules on CT images with YOLOv3: development and evaluation using simulated and patient data, Quantitative Imaging in Medicine and Surgery 10(10)(2020) 1917.